Proceeding Series of the Brazilian Society of Applied and Computational Mathematics, Vol. 5, N. 1, 2017.

Trabalho apresentado no CNMAC, Gramado - RS, 2016.

**Proceeding Series of the Brazilian Society of Computational and Applied Mathematics**

# An unstructured element based finite volume formulation for modeling viscoelastic flow

Cristiano R. Garibotti[1]
Instituto de Matemática Estatística e Física, FURG, Santo Antônio da Patrulha, RS
Clovis R. Maliska[2]
Departamento de Engenharia Mecânica, UFSC, Florianópolis, SC
Fernando S. V. Hurtado [3]
Departamento de Engenharia Mecânica, UFSC, Florianópolis, SC

**Abstract**. This work presents an element based finite volume methodology (EbFVM) [11] for solving two-dimensional viscoelastic fluid flows. The method can easily deal with hybrid unstructured meshes consisting of both triangular and quadrilateral elements, which allows the discretization of complex geometries. To overcome the problem of partial decoupling of pressure and velocity fields due to the use of a collocated arrangement of variables, it is used a interpolation function of the FIELDS type. Such a function also promoted the inclusion of pressure and stresses in the mass conservation equation improving conditioning of the coefficient matrix of the system of discretized equations. The advection terms in the constitutive equations are approximated using the single point upwind scheme. For testing different aspects of the numerical solution two classic benchmark problems were solved: flow between fixed parallel plates, and 4:1 planar contraction flow.

**Keywords**. Oldroyd-B; Element-based Finite Volume Method; Unstructured, Collocated.

## 1 Introduction

Viscoelastic fluids are used extensively in many industries such as plastic, food, electronics, oil and gas etc. Thus the numerical simulation of viscoelastic flows problems became an important research field. Over the last three decades, many important developments have been made in numerical modeling of viscoelastic flows. In the eighties and nineties, the finite element method has dominated the field of computational rheology, and most of the research was focused on the high Weissenberg number problem (HWNP), which causes numerical instability. Therefore, stabilization techniques have been used successfully by several authors. Recently, finite volume methods have been widely used for viscoelastic fluid flows. This is mainly due to its discrete conservation properties and savings in computational resources when compared to finite element methods [2, 7]. The first studies focused on solving planar contraction flow of an Oldroyd-B fluid on a non-uniform

[1]crgaribotti@furg.br
[2]maliska@sinmec.ufsc.br
[3]fernando@sinmec.ufsc.br

 

staggered grid with pressure and stress located at the center of the control volume. This arrangement avoids numerical instabilities related to the singularity at the re-entrant corner. However, staggered grids are not easily adapted to complex geometries. In order to overcome this difficulty, the co-located arrangement began to be used by several authors for both structured and unstructured meshes. In most cases the pressure-velocity-stress decoupling was removed by using the SIMPLE-like approach [2, 8] or an interpolation similar to that employed by Rhie [12].

This paper presents a finite volume method on the framework of the Element-based Finite Volume Method (EbFVM) to solve the system of governing equations of viscoelastic fluid flows. The pressure-velocity-stress decoupling is removed by using an interpolation similar to that used by Raw [11] in developing the FIELDS method for the solution of the Navier-Stokes equations on quadrilateral meshes.

## 2 Governing Equations and numerical method

Incompressible and isothermal creeping flow of a Oldroyd-B fluid in a bounded domain $\Omega \subset \mathbb{R}^2$ with external forces neglected is considered. The governing equations are represented by conservation laws for mass and momentum, in conjunction with an equation of state for stress. Since one is seeking for steady solutions at low Reynolds number, the system may be expressed in dimensionless form as:

$$\nabla \cdot \mathbf{v} = 0, \tag{1}$$

$$-\beta \nabla \cdot \nabla \mathbf{v} + \nabla p = \nabla \cdot \boldsymbol{\tau}, \tag{2}$$

$$\boldsymbol{\tau} + We \left[ \mathbf{v} \cdot \nabla \boldsymbol{\tau} - (\nabla \mathbf{v}) \cdot \boldsymbol{\tau} - \boldsymbol{\tau} \cdot (\nabla \mathbf{v})^{\mathrm{T}} \right] = (1 - \beta) \left( \nabla \mathbf{v} + (\nabla \mathbf{v})^{\mathrm{T}} \right), \tag{3}$$

where $\mathbf{v}$ is the fluid velocity, $p$ the hydrodynamic pressure, $\boldsymbol{\tau}$ is the elastic stress tensor, $\beta$ is the ratio of the retardation and relaxation times of the fluid, i.e. $\beta = \lambda_2/\lambda_1$. The non-dimensional Weissenberg number is defined by $We = \frac{\lambda_1 V}{L}$, where $V$ represents a characteristic velocity and $L$ a reference length.

As mentioned before, the above system of equations is solved using the Element-based Finite Volume Method (EbFVM) [6, 9, 11] which enabled using of unstructured hybrid grids (constituted by triangular and/or quadrilateral elements) of cell-vertex type (Figure 1). More details can be found elsewhere [3, 4, 6, 11].

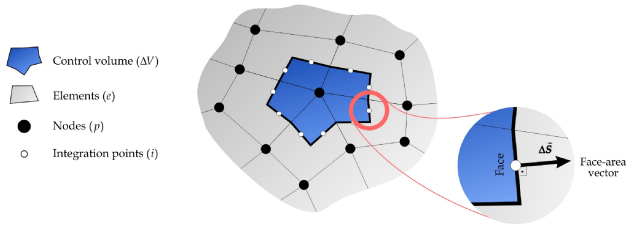


Figure 1: Main geometrical entities on the element-based finite-volume method

 

## 2.1 Discretization of governing equations

After integration of differential equations (1) - (3) over a polygonal control volume $V_p$ like the one depicted in Figure 1, they can be approximated, respectively, as

$$\sum_{e\in\mathbb{E}_p}\sum_{f\in\mathbb{F}_p^e}\mathbf{v}_{\dot{f}}\cdot\Delta\mathbf{S}_f=0, \tag{4}$$

$$-\beta\sum_{e\in\mathbb{E}_p}\left[\sum_{f\in\mathbb{F}_p^e}(\nabla\mathbf{v})_{\dot{f}}\cdot\Delta\mathbf{S}_f+\sum_{f\in\mathbb{F}_p^e}(\mathbf{P}_i^*)_{\dot{f}}\cdot\Delta\mathbf{S}_f\right]=\sum_{e\in\mathbb{E}_p}\sum_{f\in\mathbb{F}_p^e}(\boldsymbol{\tau}_i^*)_{\dot{f}}\Delta\mathbf{S}_f, \tag{5}$$

$$(\breve{\boldsymbol{\tau}})_p\,\Delta V_p+\sum_{e\in\mathbb{E}_p}\sum_{f\in\mathbb{F}_p^e}Q_f\,(\boldsymbol{\tau})_{\dot{f}}-We\left((\nabla\mathbf{v})\cdot\breve{\boldsymbol{\tau}}-\breve{\boldsymbol{\tau}}\cdot(\nabla\mathbf{v})^{\mathrm{T}}\right)_p\Delta V_p=(1-\beta)\left(\nabla\mathbf{v}+(\nabla\mathbf{v})^{\mathrm{T}}\right)_p\Delta V_p, \tag{6}$$

where $\mathbf{P}_i^*$ represents the $i^{th}$ column of the pressure tensor $\mathbf{P}$, $\boldsymbol{\tau}_i^*$ represents the $i^{th}$ column of the elastic stress tensor $\boldsymbol{\tau}$, $\Delta\mathbf{S}_f$ denotes the normal outward area vector to the control volume face $f$, as shown in Figure 1. Here $Q_f\approx\mathbf{v}_{\dot{f}}\cdot\Delta\mathbf{S}_f$ is the volumetric flow rate. In this paper, we used the diacritical mark ( $\breve{}$ ) to indicate that a given discretized variable is associated with a node. Herein $\mathbb{F}_p^e$ represents the set of control volume faces around the node $p$ located inside element $e$ and $\mathbb{E}_p$ denotes the set of all elements surrounding the control volume around node $p$. For more details concerning to the EbFVM discretization process, see references [6], [4] and [3].

## 2.2 Spatial interpolation

The discretized equations need to involve only nodal values of the unknowns. Thus, spatial interpolation schemes are needed for relating integration point values to the nodal values.

The momentum equation is an elliptic equation and a second order scheme, like bilinear shape functions [6,11], can be used safely for expressing integration point values of pressure, stress and velocity gradient as a function of correspondent nodal values.

Linear-type spatial interpolations, are not suitable for computing velocities at integration points in equation (4), because it produces unrealistic spurious spatial oscillations and unbounded values. Moreover, the absence of pressure in the continuity equation caused by collocated arrangement of the variables can result in a checkerboard problem. To overcome those problems it is employed a strategy similar to that used by Raw [11] which uses a local approximation of momentum equation at the integration point for construction of the interpolation function velocity. In this way, for the case considered here, we apply the momentum equation (2) at the face centroid, using a bilinear approximation for pressure and stress at the nodes and the approximation for the Laplacian proposed by Raw [11] we get the interpolation function for the velocity $\mathbf{v}_{\dot{f}}$:

$$\mathbf{v}_{\dot{f}}\approx\breve{\mathbf{V}}_e^{\mathrm{T}}\mathbf{N}_{\dot{f}}-\frac{L_d^2}{\beta}\mathbf{G}^{\mathrm{T}}(\breve{\mathbf{P}}_i^*)^e+\frac{L_d^2}{\beta}\mathbf{G}^{\mathrm{T}}(\breve{\boldsymbol{\tau}}_i^*)^e, \tag{7}$$

where $L_d$ is an appropriate diffusion length scale [11] and $\breve{\mathbf{V}}_e^{\mathrm{T}}$ is the matrix containing the nodal values of the velocity components.

DOI: 10.5540/03.2017.005.01.0335  

The interpolation function (7) promotes the coupling between pressure, stress and velocity fields.

Since $Q_f(\boldsymbol{\tau})_{\hat{f}}$ is an hyperbolic term, linear-type spatial interpolations are not suitable because they produce unrealistic solutions with spurious oscillations [5]. In order to avoid this, upwind-type schemes are commonly used. In this work we use the so called single point upwind (SPU) scheme, which consists of approximate the value at an interface between two adjacent volumes by the nodal value located upstream of this interface.

# 3 Results and discussion

The numerical method is first tested for solving the flow of an Oldroyd-B fluid in a simple geometry, a planar channel, for which analytical solution is easily obtained [2]. Following, a steady 4:1 contraction flow is considered. We use Picard's iterations to reduce the nonlinear problem to a sequence of linear solvers.

## 3.1 Flow in a planar channel

It is initially considered steady creeping flow of an Oldroyd-B fluid model through a planar channel, with length of $10H$ and width of $2H$, as shown in Figure 2a. The length $H$ is 1 $m$ and $V = 1$ $m/s$. The ratio $\beta$ is set to 0.2. Fully developed flow is imposed at the inlet and, due to memory effects of viscoelastic fluids, all components of the viscoelastic stress must also be prescribed. They are, $u = \frac{3}{2}(1-y^2)$, $v = 0$, $\tau_{xx} = 2We(1-\beta)\left(\partial u/\partial y\right)^2$, $\tau_{yy} = 0$, $\tau_{xy} = (1-\beta)\,\partial u/\partial y$. No-slip and permeability boundary condition are imposed at the solid boundaries. At the outflow boundary pressure is set to zero and homogeneous Neumann boundary conditions are considered for stresses. In order to demonstrate the unstructured capability of the method, simulations are carried out on the mesh shown in Figure 2b, which consist of brick elements and non-regular triangular elements. Numerical results of the stresses are shown Table 1. The $L_2$ error for the stress

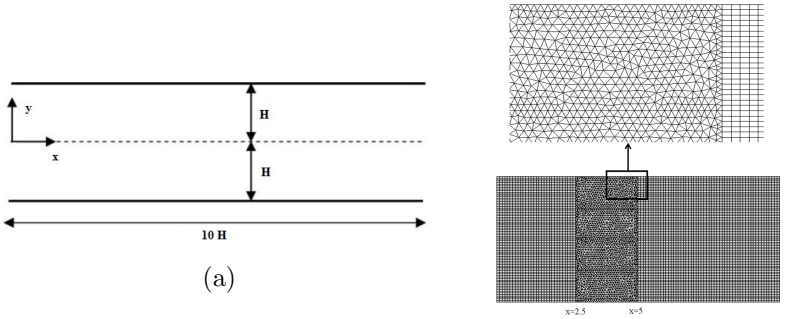


(a) (b)

Figure 2: (a) 2-D channel geometry in $xy$-plane, (b) 2-D unstructured hybrid mesh.

components are shown along cross-sections at $x = 2.5$ and $x = 5$, the delicate transition point from quadrangular to triangular elements, and at $x = 7.5$, for different values of

 

$We$. We can conclude that the agreement between the analytical and numerical solutions is very good.

Table 1: The $L_2$ errors for $\tau_{xx}$ and $\tau_{xy}$ stresses at $x = 7.5$, $x = 5$, and $x = 2.5$

| Stress | We = 0.1 | | | We = 0.3 | | |
|---|---|---|---|---|---|---|
| | x = 7.5 | x = 5 | x = 2.5 | x = 7.5 | x = 5 | x = 2.5 |
| $\tau_{xx}$ | $4.1 \times 10^{-5}$ | $2.5 \times 10^{-4}$ | $1.4 \times 10^{-4}$ | $6.2 \times 10^{-5}$ | $2.7 \times 10^{-4}$ | $1.6 \times 10^{-4}$ |
| $\tau_{xy}$ | $1.1 \times 10^{-4}$ | $3.2 \times 10^{-4}$ | $2.9 \times 10^{-4}$ | $1.8 \times 10^{-4}$ | $3.4 \times 10^{-4}$ | $2.8 \times 10^{-4}$ |
| Stress | We = 0.6 | | | We = 0.9 | | |
| | x = 7.5 | x = 5 | x = 2.5 | x = 7.5 | x = 5 | x = 2.5 |
| $\tau_{xx}$ | $1.53 \times 10^{-4}$ | $3.4 \times 10^{-4}$ | $2.4 \times 10^{-4}$ | $2.4 \times 10^{-4}$ | $4.9 \times 10^{-4}$ | $3.8 \times 10^{-4}$ |
| $\tau_{xy}$ | $2.1 \times 10^{-4}$ | $4.12 \times 10^{-4}$ | $2.7 \times 10^{-4}$ | $1.1 \times 10^{-4}$ | $4.2 \times 10^{-4}$ | $2.2 \times 10^{-4}$ |

### 3.2 The 4:1 Planar contraction flow

In this section we consider the flow of an Oldroyd-B fluid through an abrupt 4:1 planar contraction with a sharp corner. A schematic diagram of the lower half of this geometry is shown in Figure 3a. The major difficulty in the simulation of such type of problems lies in the region of contraction where the existence of a singularity point is said to cause many numerical methods to fail due to the large stresses developed in this region. A fine mesh around the corner needs to be used to capture correctly the singularity, as shown in Figure 3b. For this contraction flow simulations $V = 1/3\ m/s$ and $L = 1\ m$, so that $We = \lambda_1/3$ and the parameter $\beta$ is taken to be $1/9$. It is assumed that the downstream channel length is long enough so that the flow has a fully developed parabolic profile at the exit. At the inlet we prescribe a fully developed parabolic Poiseuille velocity profile given by $u = \frac{1}{128}(16 - y^2)$, $v = 0$. Due to memory effects of viscoelastic fluids, all components of the elastic stress must be prescribed, that is $\tau_{xx} = We\,(1-\beta)\frac{1}{2048}y^2$, $\tau_{yy} = 0$, $\tau_{xy} = -(1-\beta)\frac{1}{64}y$. At the outflow, pressure is set to zero. No-slip conditions are imposed on solid walls for $u$ and $v$ and symmetry conditions are specified on axis of symmetry.

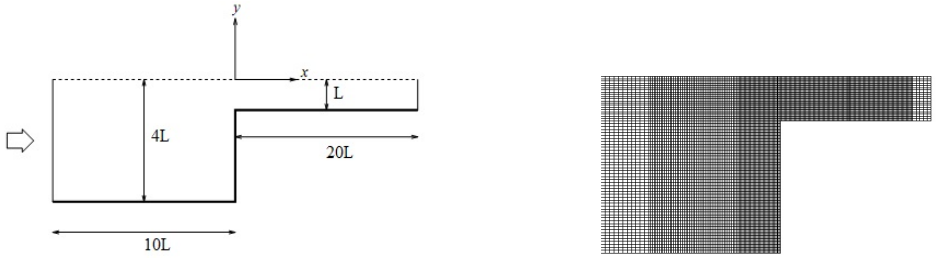


(a) (b)

Figure 3: (a) Contraction flow geometry. (b) Contraction flow mesh

Figures 4a, 4b, and 4c present the evolution of the stress components along the line $y = -1$ for different values of $We$. As we can see, the stress components attains their maximum at the re-entrant corner. For the second and third components of the stress

DOI: 10.5540/03.2017.005.01.0335  

tensor the curves are quasi-identical and are independent of Weissenberg number, which is expected [7]. Contour plots of the stress components are presented in Figures 4d, 4e,

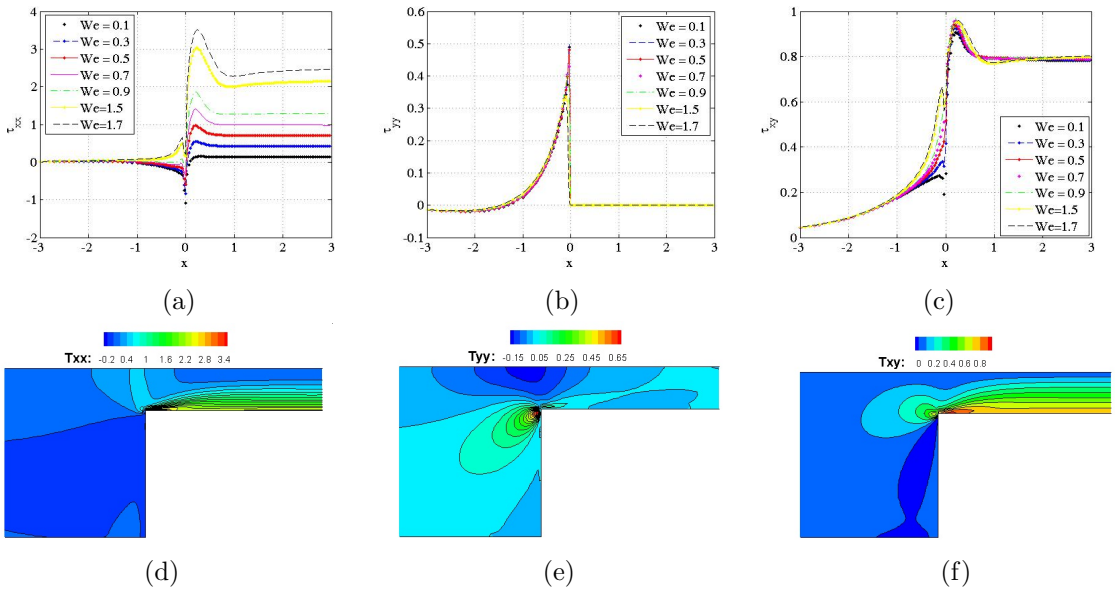


Figure 4: Stresses profiles along the line $y = -1$ for a range of values of $We$: (a) $\tau_{xx}$ stress component, (b) $\tau_{yy}$ stress component, (c) Shear stress $\tau_{xy}$. Stress contours for $We = 1.7$: (d) $\tau_{xx}$ stress component, (e) $\tau_{yy}$ stress components, (f) Shear stress $\tau_{xy}$

and 4f for $We = 1.7$, which is the maximum value of Weissenberg number achieved in our computations. The stress contours are smooth around the corner singularity, while stress boundary layers develop downstream of the re-entrant corner. It is also observed a high stress concentration for $\tau_{xx}$ and $\tau_{xy}$ at the wall just after downstream the re-entrant corner. These findings are in close correspondence with those found in references [1, 2, 7, 10].

## 4 Conclusions

The numerical methodology presented in this paper has contributed for the theoretical development of the EbFVM for solving viscoelastic fluid flow problems. The approach of using a unique numerical method for the solution of both constitutive equations and conservation of mass and momentum equations, and the new interpolation function for approximating velocities at the integration points in the mass conservation equation facilitates the pressure-velocity-stress coupling as well as the development of the computational code. The ability of solving different physics with the same numerical method is a strong point in favor of the EbFVM method.

DOI: 10.5540/03.2017.005.01.0335  

## References

[1] M. Aboubacar and M. F. Webster. A cell-vertex finite volume/element method on triangles for abrupt contraction viscoelastic flows. *Journal of Non-Newtonian Fluid Mechanics*, 98(23):83–106, 2001.

[2] S. S. Edussuriya, A. J. Williams, and C. Bailey. A cell-centred finite volume method for modelling viscoelastic flow. *Journal of Non-Newtonian Fluid Mechanics*, 117(1):47–61, 2004.

[3] C. R. Garibotti. *Uma metodologia de volumes finitos para a resolução de escoamentos viscoelásticos com malhas não-estruturadas híbridas.* PhD thesis, Departamento de Engenharia Mecânica, UFSC, Florianópolis, 2014.

[4] F S V Hurtado. *Formulação tridimendional de volumes finitos para a Simulação de reservatórios de petróleo com malhas não-estruturadas.* PhD thesis, Departamento de Engenharia Mecânica, UFSC, Florianópolis, 2011.

[5] F. S. V. Hurtado, Maliska C. R., and A. F. C. Silva. Application of flux-correted transport to an unstructured-grid finite-volume formulation for reservoir simulation. In *Proceedings of the XXVIII CILANCE*, 2007.

[6] C. R. Maliska. *Transferência de calor e mecânica dos fluidos computacional.* LTC, 2 edition, 2004.

[7] L. Nadau and A. Sequeira. Numerical simulations of shear dependent viscoelastic flows with a combined finite element–finite volume method. *Comput. Math. Appl.*, 53(3-4):547–568, 2007.

[8] P. J. Oliveira and F. T. Pinho. Plane contraction flows of upper convected Maxwell and Phan-Thien-Tanner fluids as predicted by a finite-volume method. *Journal of Non-Newtonian Fluid Mechanics*, 88(12):63–88, 1999.

[9] S. V. Patankar. *Numerical Heat Transfer and Fluid Flow.* Series in computational methods in mechanics and thermal sciences. Hemisphere Publishing Corporation, 1980.

[10] T. N. Phillips and A. J. Williams. Comparison of creeping and inertial flow of an Oldroyd–B fluid through planar and axisymmetric contractions. *Journal of Non-Newtonian Fluid Mechanics*, 108(13):25–47, 2002.

[11] M. J. Raw. *A new control-volume based finite element procedure for the numerical solution of the fluid flow and scalar transport equations.* PhD thesis, 1985.

[12] C. M. Rhie and W. L. Chow. Numerical study of the turbulent flow past an airfoil with trailing edge separation. *AIAA Journal*, 21:1525–1532, November 1983.

DOI: 10.5540/03.2017.005.01.0335  